An Approximate PML Applied to Cylindrical and Spherical Coordinate Sectors

doi: 10.1109/LMWC.2018.2853565

An Approximate PML Applied to Cylindrical and Spherical Coordinate Sectors

Yoshiaki Ando, *Member, IEEE,*

***Abstract*—This paper proposes an approximate perfectly matched layer (PML) that is applicable to cylindrical and spherical coordinate sectors. The proposed PML is based on complex coordinate stretching, which enables the truncation of FDTD grids, not only at ρ- and r- coordinates, but also at ϕ- and θ- coordinates. The absorption performance of the PML is demonstrated through numerical simulations.**

***Index Terms*—Perfectly matched layer, complex coordinate stretching.**

I. Introduction

PERFECTLY matched layer (PML) [1] has been widely used as a standard absorbing boundary condition to truncate a computational domain for solving open-region problems by using the finite-difference time-domain (FDTD) method. The PML based on complex coordinate stretching facilitates PML formulation in the framework of Maxwell's equations [2]. Although the FDTD method has been applied to various coordinate systems, studies on the development of PML for such systems are rather limited. Among the seminal works on the PML based on complex coordinate stretching, Teixeira and Chew [3] formulated cylindrical (ρ, ϕ, z) and spherical (r, θ, ϕ) PMLs with complex coordinate stretching, where waves propagating in the ρ- and z-directions, and r-direction are absorbed in the cylindrical and spherical coordinates, respectively. The above mentioned PMLs are useful for solving scattering problems with cylindrical and spherical symmetry; however, problems characterized by limited regions wherein a computational domain is truncated in constant ϕ- and θ-planes still remains a challenge. An example of such a problem is propagation in an earth-ionosphere waveguide in very-low-frequency (VLF) or low-frequency (LF) bands, where it is sufficient to simulate fields only in the region along a propagation path [5].

This paper, therefore, proposes an approximate PML formulation that is applicable to cylindrical and spherical sectors, in which a computational region is truncated at constant azimuthal and polar coordinates as well as radial coordinates. The proposed method is based on complex coordinate stretching; however, the variable change is not fully considered and some parts of the coordinate remain unchanged. To implement complex coordinate stretching in the time domain, auxiliary field variables must be introduced. The proposed method reduces the auxiliary fields to mitigate increases in computational costs while maintaining the performance of the PML.

Manuscript received September 15, 2017; revised January 25, 2018 and June 6, 2018; accepted June 27, 2018. This work was supported by JSPS KAKENHI Grant Number JP26420224, JP17K06295 and the Telecommunications Advancement Foundation.

The author is with the Department of Informatics and Communication Engineering, Graduate School of Informatics and Engineering, The University of Electro-Communications, Chofu, Tokyo, 1828585 Japan (e-mail: y-ando@uec.ac.jp)

II. Formulation

A. PML in cylindrical coordinates

In this section we describe the PML applied to computational domain having the form of a cylindrical sector for the two-dimensional TM$_z$ case. To accomplish this, in addition to the coordinate stretching in the ρ-direction [3], we introduce stretching in the ϕ-direction normal to the boundary of the sector. The three-dimensional formulation is rather straightforward because the z-axis is the same as that in the Cartesian system.

The complex stretched variable transformations with respect to α can be represented as follows.

$$\alpha \to \tilde{\alpha} = \int_{\alpha_0}^{\alpha} s_\alpha(\alpha')d\alpha' + \alpha_0 = \alpha - j\frac{\tilde{\sigma}_\alpha}{\omega}, \tag{1}$$

where $\alpha = \rho$ and ϕ; α_0 is a constant; $s_\alpha = 1 - j\sigma_\alpha(\alpha)/\omega$; and $\tilde{\sigma}_\alpha = \int_{\alpha_0}^{\alpha} \sigma_\alpha(\alpha')d\alpha'$. It is known that the coordinate ϕ is not a measure of length; therefore, Eq. (1) with $\alpha = \phi$ can be considered as the transformation of the variable $\rho\phi$ to $\rho\tilde{\phi}$.

Maxwell's equations can then be rewritten as follows:

$$j\omega\varepsilon E_z = \frac{1}{\tilde{\rho}}\frac{1}{s_\rho}\frac{\partial(\tilde{\rho}H_\phi)}{\partial\rho} - \frac{1}{\tilde{\rho}}\frac{1}{s_\phi}\frac{\partial H_\rho}{\partial\phi}, \tag{2}$$

$$j\omega\mu H_\rho = -\frac{1}{\tilde{\rho}}\frac{1}{s_\phi}\frac{\partial E_z}{\partial\phi}, \tag{3}$$

$$j\omega\mu H_\phi = \frac{1}{s_\rho}\frac{\partial E_z}{\partial\rho}, \tag{4}$$

Here, we adopt the time factor $e^{j\omega t}$. In a manner similar to [2], the time domain equations to be solved are represented as

$$\frac{\partial\tilde{E}_{z\rho}}{\partial t} + \sigma_\rho\tilde{E}_{z\rho} = \frac{1}{\varepsilon}\frac{\partial\tilde{H}_\phi}{\partial\rho}, \tag{5}$$

$$\frac{\partial\tilde{E}_{z\phi}}{\partial t} + \sigma_\phi\tilde{E}_{z\phi} = -\frac{1}{\varepsilon}\frac{\partial H_\rho}{\partial\phi}, \tag{6}$$

$$\tilde{E}_z = \tilde{E}_{z\rho} + \tilde{E}_{z\phi}, \tag{7}$$

$$\rho\frac{\partial E_z}{\partial t} + \tilde{\sigma}_\rho E_z = \frac{\partial\tilde{E}_z}{\partial t}, \tag{8}$$

$$\frac{\partial\tilde{H}_\rho}{\partial t} + \sigma_\phi\tilde{H}_\rho = -\frac{1}{\mu}\frac{\partial E_z}{\partial\phi}, \tag{9}$$

$$\frac{\partial H_\phi}{\partial t} + \sigma_\rho H_\phi = \frac{1}{\mu}\frac{\partial E_z}{\partial\rho}, \tag{10}$$

$$\rho\frac{\partial H_\rho}{\partial t}+\tilde{\sigma}_\rho H_\rho=\frac{\partial \tilde{H}_\rho}{\partial t}, \tag{11}$$

$$\frac{\partial \tilde{H}_\phi}{\partial t}=\rho\frac{\partial H_\phi}{\partial t}+\tilde{\sigma}_\rho H_\phi. \tag{12}$$

Note that the field variables on the left-hand side of the above equations must be updated by finite differentiation. Therefore, for the time-domain solution, it is necessary to introduce the following auxiliary field variables: $\tilde{E}_{z\rho}, \tilde{E}_{z\phi}, \tilde{E}_z, \tilde{H}_\rho$, and $\tilde{H}_\phi$.

B. Simplified PML in cylindrical coordinates

The second term on the right-hand side in Eq. (2) and Eq. (3) absorb the wave components propagating along the ϕ-direction. These terms influence the PML normal to ϕ where $s_\phi \neq 1$ and $s_\rho = 1$. Therefore, the operator $\frac{1}{\tilde{\rho}s_\phi}\frac{\partial}{\partial\phi}$ can be approximated by $\frac{1}{\rho s_\phi}\frac{\partial}{\partial\phi}$. This approximation would affect only the four corners of FDTD grids where PMLs normal to the ρ- and ϕ-axes are overlapped. For example, Eq. (2) becomes

$$j\omega\varepsilon E_z=\frac{1}{\tilde{\rho}}\frac{1}{s_\rho}\frac{\partial(\tilde{\rho}H_\phi)}{\partial\rho}-\frac{1}{\rho}\frac{1}{s_\phi}\frac{\partial H_\rho}{\partial\phi}. \tag{13}$$

In the time domain, Eqs. (6), (7), and (9) are rewritten as

$$\frac{\partial E_{z\phi}}{\partial t}+\sigma_\phi E_{z\phi}=-\frac{1}{\varepsilon}\frac{1}{\rho}\frac{\partial H_\rho}{\partial\phi}, \tag{14}$$

$$E_z=E_{z\rho}+E_{z\phi}, \tag{15}$$

$$\frac{\partial H_\rho}{\partial t}+\sigma_\phi H_\rho=-\frac{1}{\mu}\frac{1}{\rho}\frac{\partial E_z}{\partial\phi}. \tag{16}$$

Moreover, $E_{z\rho}$ must be updated before the operation of Eq. (15) by

$$\rho\frac{\partial E_{z\rho}}{\partial t}+\tilde{\sigma}_\rho E_{z\rho}=\frac{\partial\tilde{E}_{z\rho}}{\partial t}, \tag{17}$$

and thus, Eq. (8) is rendered redundant. In this formulation, the number of update equations decreases by one whereas that of the auxiliary field variables reduces to the following four, $\tilde{E}_{z\rho}, E_{z\rho}, E_{z\phi}$, and $\tilde{H}_\phi$.

C. Simplified PML in spherical coordinates

In the spherical coordinates, a similar formulation is prescribed, as follows. The coordinate transformation is the same as Eq. (1). As stated earlier, the coordinate transformation can be considered as $r\theta$ to $r\tilde{\theta}$ and $r\sin\theta\phi$ to $r\sin\theta\tilde{\phi}$. As a result, the Maxwell-Ampere's law can be rewritten as

$$\frac{1}{r}\frac{1}{s_\theta}\frac{\partial H_\phi}{\partial\theta}+\frac{\cot\theta}{r}H_\phi-\frac{1}{r\sin\theta}\frac{1}{s_\phi}\frac{\partial H_\theta}{\partial\phi}=j\omega\varepsilon E_r, \tag{18}$$

$$\frac{1}{r\sin\theta}\frac{1}{s_\phi}\frac{\partial H_r}{\partial\phi}-\frac{1}{\tilde{r}}\frac{1}{s_r}\frac{\partial(\tilde{r}H_\phi)}{\partial r}=j\omega\varepsilon E_\theta, \tag{19}$$

$$\frac{1}{\tilde{r}}\frac{1}{s_r}\frac{\partial(\tilde{r}H_\theta)}{\partial r}-\frac{1}{r}\frac{1}{s_\theta}\frac{\partial H_r}{\partial\theta}=j\omega\varepsilon E_\phi, \tag{20}$$

In addition, the transformation of Faraday's law is similar according to the duality of Maxwell's equations. In Eq. (18), to improve absorption performance, the equation mapped onto the stretched coordinate space is $\frac{1}{r}\frac{\partial H_\phi}{\partial\theta}+\frac{\cot\theta}{r}H_\phi$ as opposed to $\frac{1}{r\sin\theta}\frac{\partial}{\partial\theta}(\sin\theta H_\phi)$. It is noted that the r-coordinate is not transformed in terms of differentiation with respect to θ and ϕ, as discussed in the previous section.

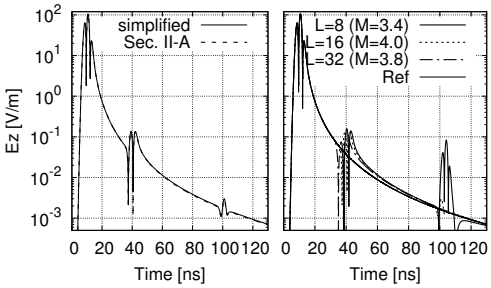

Fig. 1. Left panel: Numerical results obtained from the formulas in Secs. II-A and II-B. Right panel: Observed waveforms with varying numbers of sublayers.

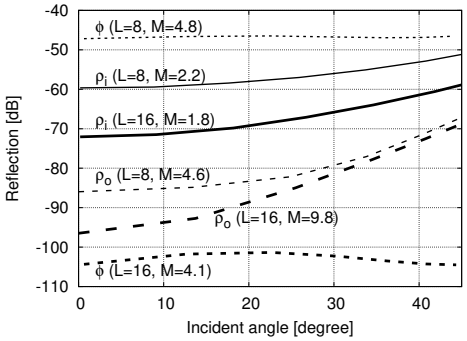

Fig. 2. Dependence of reflection from PML on the incident angle

The update equations in the time domain are obtained in the same manner as in the case of cylindrical coordinates, where the r-components of the curl equations are split into three components corresponding to the terms on the left-hand side of Eq. (18), and H_ϕ is the averaged value of neighboring fields because it is not assigned to the staggered Yee cell.

For computation in the PML region, twenty-two auxiliary field variables are necessary— twelve split subcomponents, two are further split as shown in Eq. (18); the remaining eight variables are $\tilde{E}_{\theta r}$, $\tilde{E}_{\phi r}$, $\tilde{H}_{\theta r}$, $\tilde{H}_{\phi r}$, $\tilde{E}_\theta$, $\tilde{E}_\phi$, $\tilde{H}_\theta$, and $\tilde{H}_\phi$.

III. NUMERICAL RESULTS

A. Cylindrical PML

For evaluating the reflection of the developed PML, the waveforms are measured at an observation point. The computational domain is defined by $\rho_i \leqq \rho \leqq \rho_o (= \rho_i + R_\rho)$ and $0 \leqq \phi \leqq \phi_0$, where $\rho_i = 21.2$, $R_\rho = 25.6$, and $\phi_0 = 5\pi/8$. The domain is discretized by $N_\rho \times N_\phi = 640 \times 1000$ cells. The temporal step is chosen as $\Delta t = 0.99/c_0/\sqrt{\Delta\rho^{-2} + (\rho_i\Delta\phi)^{-2}}$, where c_0 is the speed of light in vacuum. The PML with L-sublayers lies inside the domain. Moreover, the fields are excited by a current source with current density J_z [A/m^2] at (ρ_s, ϕ_s), spread over an area corresponding to one cell $\Delta S (= \Delta\rho \times \rho_s\Delta\phi)$; here, $\rho_s = 27$ and $\phi_s = 3\pi/16$. The waveform of $J_z\,\Delta S$, defined as $f(t)$, is given by

$$f(t) = -\frac{t-t_0}{\sigma}\exp\left(-\frac{\{t-t_0\}^2}{2\sigma^2}\right), \tag{21}$$

where $\sigma = 12\Delta t$ and $t_0 = 6\sigma$. The observation point is located at $\rho_1 = 26, \phi_1 = \phi_s$, and $L = 16$. The absorption parameters σ_ρ and σ_ϕ are chosen as $\sigma(\alpha) = -\{\alpha/(L\,\Delta\alpha)\}^M(M +$

$1)c_0 \ln R_0/(2L\Delta\alpha)$, where α is the distance from the interface between PML and the vacuum, and $\Delta\alpha$ is the cell size.

Figure 1 shows the numerical results of $|E_z|$ obtained using the proposed PML. The left panel illustrates the difference between the results obtained using the simplified equations discussed in Sec. II-B(solid line) and the equations formulated in Sec. II-A(the broken line). The direct wave is observed at approximately 10 ns, and the reflected waves are observed at approximately 40 and 100 ns; the former is the wave reflected from the PML near $\rho = \rho_i$, while the latter is the wave reflected from the PML near $\phi = 0$. Both the results coincide with each other, indicating that the simplified formulation is effective. It should be noted that the use of simplified equations decreases the computational time required for updating H_ρ by a factor of 1.5.

The right panel illustrates the waveforms of $|E_z|$ computed using the simplified formulas in Sec. II-B for the number of sublayers $L = 8, 16$, and 32. The location of the observation point is the same as in the previous case. The curve labeled as "Ref" is obtained by setting a large computational domain such that the reflected waves from the grid boundaries are not observed. We see that the reflected wave at $t = 100$ ns, which corresponds to the reflection from the PML near $\phi = 0$, is sufficiently mitigated for $L = 16$. In contrast, the reflection observed at $t = 40$ ns, corresponding to the reflection from the PML near $\rho = \rho_i$, is not mitigated effectively (-47.7 dB) despite the increase in L.

Figure 2 shows the reflection from the simplified PML for $L = 8$ and 16, as a function of the incident angle. Here, ρ_i and ρ_o denote the convex and concave PMLs, respectively, and ϕ denotes the PML normal to ϕ-direction. The Fourier transform of FDTD results are taken and then normalized by the amplitude of waves propagating with the same distance as the reflected waves, at the frequency corresponding to the sampling number $N_s = 15$, i.e., the wavelength equal to 15 cells. Although the reflection from the convex PML is relatively higher, we can conclude that the developed PML is effective.

B. Spherical PML

The computational domain for measuring spurious reflections from the proposed PML is defined as $r_i \leqq r \leqq r_o$, $\theta_1 \leqq \theta \leqq \theta_2$, and $0 \leqq \phi \leqq \phi_2$, where $r_i = 3.2, r_o = 7.4$, $\theta_1 = \left(\frac{1}{2} - \frac{9}{32}\right)\pi, \theta_2 = \left(\frac{1}{2} + \frac{9}{32}\right)\pi$, and $\phi_2 = 3\pi/4$. This domain is discretized into $N_r \times N_\theta \times N_\phi = 210 \times 225 \times 300$ cells, i.e., $\Delta r = (r_o - r_i)/N_r = 0.02$, and $\Delta\theta = \Delta\phi = \pi/400$; the temporal step is $\Delta t = 0.999/c_0/\sqrt{(\Delta r)^{-2} + (r_i\,\Delta\theta)^{-2} + (r_i \sin\theta_1\,\Delta\phi)^{-2}}$. A current with dipole moment $J_\theta \Delta V$ [A·m] $= f(t)$ in Eq. (21) is located at $(r_s, \theta_s, \phi_s) = (5, \pi/2, 3\pi/8)$ for excitation.

Figure 3 indicates the waveform of $|E_\theta|$ observed at $(r', \theta', \phi') = (4.5, \pi/2, 3\pi/8)$ with $L = 4, 8$, and 16 sublayers, and $M = 2.5$, 3.6, and 3.7, respectively. The results were computed using the simplified formulas presented in Sec. II-C. The direct wave from the source is observed at approximately 4 ns, and the reflected waves are observed at approximately 13, 20, 27, and 34 ns. Through numerical simulations, we

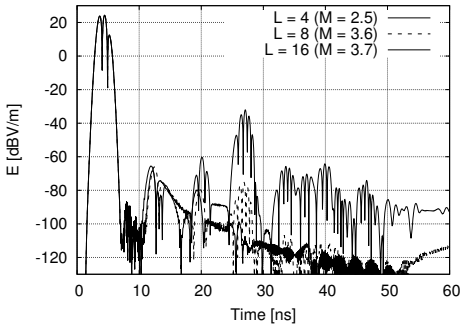

Fig. 3. Observed waveform (direct and reflected waves from boundaries) corresponding to various PML sublayers L

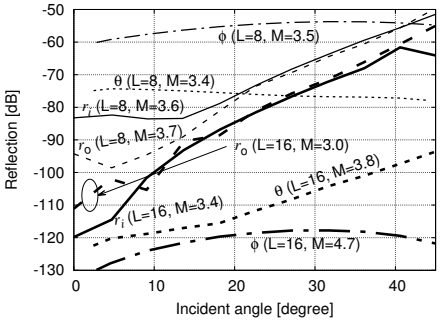

Fig. 4. The dependence of reflection on the incident angle from the spherical PML. The sampling number $N_s = 15$.

can confirm that the wave at approximately 13 ns is reflected from the PML near $r = r_i$, and similarly, the waves at approximately 20, 27, and 34 ns correspond to the PML near $r = r_o$, $\theta = \theta_{1,2}$, and $\phi = \phi_{1,2}$, respectively. We can see that an increase in the sublayers mitigates the reflections down to the given reflection coefficient $R_0 = 10^{-6}$.

In Fig. 4, the dependence of the reflection of the spherical PML on the incident angle is illustrated for $L = 8$ and 16. From the results, we see that the spherical PML developed in this work demonstrates excellent absorption performance.

IV. Conclusion

In this work, we proposed a novel PML formulation that can be applied to cylindrical and spherical sectors as FDTD grids. The numerical results confirm the proposed PML has adequate absorption performance. In addition, we also developed a simplified formulation of the PML, which was demonstrated to exhibit identical performance.

References

[1] J.-P. Berenger, "Perfectly matched layer for absorption of electromagnetic waves," J. Comp. Phys., vol. 114, pp. 185-200, 1994.

[2] W. C. Chew and W. H. Weedon, "A 3-D perfectly matched medium from modified Maxwell's equations with stretched coordinates," Microwave Opt. Tech. Lett., vol. 7, no. 13, pp. 599-604, 1994.

[3] F. L. Teixeira and W. C. Chew, "PML-FDTD in cylindrical and spherical grids," IEEE Microwave Guided Wave Lett., vol. 7, no. 9, pp. 285-287, 1997.

[4] R. Holland, "THREDS: A finite-difference time-domain EMP code in 3D spherical coordinates," IEEE Trans. Nucl. Sci., vol. 30, pp. 4592-4595, 1983.

[5] L. Zhou, X. Xi, and Y. Du, "Application in low-frequency ground-wave propagation of parallel FDTD based on GPU," 2012 10th International Symp. Antennas, Propagation & EM Theory (ISAPE), 22-26 Oct. 2012.